Atmos. Chem. Phys. Discuss., 10, 5135–5184, 2010
www.atmos-chem-phys-discuss.net/10/5135/2010/

Atmospheric Chemistry and Physics Discussions

A modelling study of air quality impact of odd-even day traffic restriction scheme before, during and after the 2008 Beijing Olympic Games

H. Cai and S. D. Xie

College of Environmental Science and Engineering, State Key Joint Laboratory of Environmental Simulation and Pollution Control, Peking University, Beijing, China

Received: 24 November 2009 – Accepted: 10 February 2010 – Published: 23 February 2010

Correspondence to: S. D. Xie (sdxie@pku.edu.cn)

Published by Copernicus Publications on behalf of the European Geosciences Union.

Abstract

Systematic air pollution control measures were designed and implemented to improve air quality for the 2008 Beijing Olympics. This study focuses on the evaluation of the air quality impacts of a short-term odd-even day traffic restriction scheme (TRS) implemented before, during and after the Games, based on modelling simulation by a well validated urban-scale air quality model. Concentration levels of CO, PM_{10}, NO_2 and O_3 were predicted for the pre- (10–19 July), during- (20 July–20 September) and post-TRS (21–30 September) periods, based on the on-line monitored traffic flows on a total of 334 road segments constituting the 2nd, 3rd, 4th Ring Roads (RR) and the major Linkage Roads (LRs) that were subject to the TRS policy and distributed around the main urban area of Beijing, and on the hourly sequential meteorological data from a representative Observatory. Subsequently, we used the predictions and observations at a roadside air quality monitoring site to evaluate the model, based on a widely used statistical framework for model evaluation, as well as on the dependence of model performance on time-of-the-day and on wind direction, and the model predictions turned out satisfactory. Results showed that daily average concentrations on the 2nd, 3rd, 4th RR and LRs during the TRS period decreased significantly, by about 35.8%, 38.5%, 34.9% and 35.6% for CO, about 38.7%, 31.8%, 44.0% and 34.7% for PM_{10}, about 30.3%, 31.9%, 32.3% and 33.9% for NO_2, and about 36.7%, 33.0%, 33.4% and 34.7% for O_3, respectively, compared with the pre-TRS period. Besides, hourly average concentrations were also reduced significantly, particularly for the morning and evening peaks for CO and PM_{10}, for the evening peak for NO_2, and for the afternoon peak for O_3. Consequently, both the daily and hourly concentration level of CO, PM_{10}, NO_2 and O_3 conformed to the CNAAQS (China National Ambient Air Quality Standards) Grade II during the Games. Besides, a notable ozone weekend effect was revealed for the pre- and post-TRS periods, and was virtually removed for the during-TRS period. In addition, notable reduction of concentration levels were achieved in different regions of Beijing in response to the TRS policy, with the air quality in the downwind northern and

ACPD

10, 5135–5184, 2010

western regions improved most significantly. The TRS policy was therefore effective in improving short-term air quality in Beijing during the Games.

1 Introduction

Beijing, the capital city of China and the host city of the 2008 Olympic Games, has a population of over 18 million and meanwhile suffers serious air pollution constituted by high concentration levels of PM_{10}, CO, SO_2 and NO_2. Particularly, PM_{10}, with its high daily and annual concentrations on average, remained the primary air pollutant in Beijing since 2000 (Beijing EPB, 2009). The PM_{10} annual average concentration in Beijing has been staying at a high level, fluctuating around 160 µg/m^3 during the period of 2001–2006, and began to decrease in the following two years as a result of various control measures, with the annual average concentration in 2008 still exceeding 120 µg/m^3 (Beijing EPB, 2009), which was about 20% higher than the China National Ambient Air Quality Standards (CNAAQS) Grade II (100 µg/m^3) and six times the latest World Health Organization (WHO) Air Quality Guidelines (WHO, 2005). Of the major anthropogenic sources of atmospheric particulate matters in the mega cities (e.g. Beijing, Shanghai, Guangzhou) in China, on-road vehicular emissions is an important and perhaps the fastest growing one (Chan and Yao, 2008). Although the source contributions of motor vehicles to PM_{10} and $PM_{2.5}$ in Beijing revealed by the PMF (positive matrix factorization) methodology were only 5% (Xie et al., 2008) and 6% (Song et al., 2006), respectively, motor vehicles were a major contributor to ambient concentrations of nitrogen dioxide (NO_2)/nitrogen oxides (NO_x) and carbon monoxide (CO), according to a conclusion that on-road vehicle source had contributed 76.5% and 68.4% of the CO and NO_x concentrations, respectively, in urban atmosphere of Beijing in 1995 (Hao et al., 2001). Moreover, traffic congestion and traffic-related air pollution has been a serious issue in urban Beijing with the vehicle population increasing dramatically at a daily rate of over one thousand, reaching over 3.5 million by the end of 2008. The booming economic prosperity and substantial increase of vehicle population has resulted in the exponential growth of vehicular emissions of CO, PM_{10}, NO_x, VOC (volatile organic compounds) (Cai and Xie, 2007), as well as speciated VOC emissions containing highly reactive and toxic pollutants in the atmosphere of Beijing (Cai and Xie, 2009). In order to improve effectively the air quality and traffic condition in Beijing, a Sino-Italian environmental protection program based on Intelligent Traffic System and Traffic Air Pollution (ITS-TAP) monitoring was launched between the Italian Ministry for the Environment and Territory and Beijing Municipal Government in 2005. Moreover, the Beijing Municipal Government had committed to the international society that air quality in Beijing would be improved and be better than before, satisfying the CNAAQS and WHO Air Quality Guidelines during the 2008 Olympic Games. To fulfill the air quality commitment during the Games, the government implemented a list of control measures, including six control schemes for vehicular emissions: issuance of new automobile emissions standards; decommissioning of high emissions vehicles, buses and taxis; recovery of fuel vapors at pumping stations and from tankers; restricted use of high emissions vehicles; banning of large polluting vehicles from the roads; control of emissions from small stationary diesel generators (COC, 2008). Meanwhile, Beijing took the lead in China to adopt the Euro-IV emission standard to reduce vehicle emissions of air pollutants five months before the Olympic Games. Particularly, an odd-even day traffic restriction scheme (TRS), a control measure that was demonstrated to be effective in Atlanta (Fang et al., 2009), was enforced for two months from 20 July to 20 September 2008, to help ease congestion and improve air quality during the Olympics and Paralympics. Previously, Cheng et al. (2008) demonstrated that the four-day traffic restrictions in Beijing during the Sino-African Summit in early November 2006 resulted in significant temporary reductions in concentrations of NO_x and particulates in the city. Besides, Westerdahl et al. (2009) conducted in-situ measurement and concluded that a four-day traffic control experiment from 17–20 August 2007 conducted by the Beijing Government as a pilot to test the effectiveness of the proposed odd-even day TRS was effective in reducing extreme concentrations that occurred at both on-road and ambient environments. Wang et al. (2009a) evaluated the air quality impacts of the 2008 Beijing

Olympic Games, focusing on the measurement of on-road black carbon emission factors and the evaluation of reduction of black carbon concentrations. Wang et al. (2009b) conducted a modelling analysis, aiming to assess the effectiveness of various emission restrictions implemented during the 2008 Beijing Olympics on the ozone air quality at a rural site of Beijing during the period. This study, based on a modelling simulation with online-monitored data of on-road traffic flows at a high temporal resolution of two seconds from the ITS-TAP system, focuses on the evaluation of the effectiveness of the odd-even day TRS implemented before, during and after the Games on air quality improvement around the urban areas of Beijing (UAB).

Model-based simulation has been one of the major tools for air quality assessment, air pollution diagnosis and evaluation of pollution control policies at the urban, regional and global levels. A few dispersion models have been widely applied to simulate urban air pollution from traffic-related emissions, e.g. OSPM (Berkowicz, 2000; Kukkonen et al., 2001; Assael et al., 2008; Berkowicz et al., 2008), CALINE (Levitin et al., 2005; Yura et al., 2007), CALPUFF (Wang et al., 2006), ISCST3 (Elbir, 2002; Ying et al., 2007; Sharma and Chandra, 2008). ADMS-Urban, a well tested and intensively validated quasi-Gaussian dispersion air quality model, which is widely used for regulatory purposes in the UK and used in the investigation and assessment of air pollution mitigation and control strategies in many cities of China (Carruthers et al., 1994; Bennett and Hunter, 1997; McHugh et al., 1997; Carruthers et al., 1999; Carruthers et al., 2000a; Carruthers et al., 2001; Riddle et al., 2004; McHugh et al., 2005; Hirtl and Baumann-Stanzer, 2007), has recently been validated by the Ministry of Environmental Protection of China as one of the three recommended dispersion models (the others are the US EPA's CALPUFF and AERMOD) for air quality impact assessment (MEPC, 2009), and by a commercial system of street-level air quality forecasting which was launched in Beijing in July 2008 (BeijingAir, 2008). Thus, ADMS-Urban was adopted in this study to simulate and assess the air quality impact in UAB in response to the TRS policy before, during and after the 2008 Beijing Olympic Games. Firstly, the modelled results were evaluated with the measurement data from a roadside air quality monitoring site. Subsequently, the ambient concentrations of CO, PM_{10}, NO_2 and O_3 at a height of 1.5 m resulting from motor vehicles along the 2nd, 3rd and 4th Ring Roads (RR) and Linkage Roads (LRs, including major intercity expressways and intercity roads between RRs) distributed within UAB were calculated for the periods of pre-TRS (10–19 July 2008), during-TRS (20 July–20 September 2008) and post-TRS (21–30 September 2008), respectively, followed by an assessment of the temporal and spatial variation of air quality impacts in response to the TRS policy.

2 Methods and data

2.1 Description of study domain, urban and background monitoring sites and receptors

The study domain, the main UAB, covers the 2nd, 3rd and 4th RR, which were 32.7, 48.0 and 65.3 kilometers long, and had six, six to eight and eight lanes, respectively, as well as the major LRs mainly having eight lanes. About 62% of Beijing is mountainous area located in the west, the north and the northeast. Thus, the local wind field has a clear diurnal variation, with southeasterly wind dominating in the daytime and northerly wind dominating in the night. The Chegongzhuang (CGZ) air quality monitoring site, which was located five kilometers west of the West 2nd RR and was on a corner (geographical coordinates: 39°55′53″ N, 116°19′38″ E) of a crossroad where a five-lane North-South oriented street and a six-lane West-East oriented street intersected with high traffic flows, had a sampling height of about 4.5 m from ground and had been well maintained with routine calibration of the measurement equipment by the Beijing Municipal Environmental Monitoring Centre during the Games as a traffic monitoring site. This site provided the model evaluation data of hourly concentrations of CO, PM_{10}, NO_2 and O_3 for 10–20 July and 10–20 August 2008. The Dingling (DL) background monitoring station, which was approximately 42 kilometers north from the CGZ air quality monitoring site and was in the suburban area with very few motor vehicles, provided

ACPD
10, 5135–5184, 2010

background diurnal profiles for CO, PM_{10} and NO_2 for the whole evaluation period, to assure that the modelling results with consideration of background measurement from DL would reflect well the real situation of the air quality in the UAB during the Games, which was expected to be influenced mainly by local on-road vehicles, with a minor contribution from other well controlled sources like power plants and polluting industrial plants, construction sites and gas stations both in Beijing and the surrounding provinces during the Games (Wang et al., 2009). Therefore, it is reasonable to make comparisons between modelled predictions and measurement data at CGZ for the model evaluation. For O_3, a major secondary air pollutant, we used the measurement data from Shangdianzi (SDZ) regional atmospheric background monitoring site, one of the four regional atmospheric background monitoring sites in China and located about 150 kilometres northeast of Beijing (40°39′ N, 117°07′ E). Measurement data from the SDZ background measurement site are free of influence by motor vehicles and represent the background characteristic of atmospheric constitutes in northern regions of China including Beijing (Liu et al., 2007). Therefore, this site is suitable for providing the background O_3 measurement data for this modelling study. Due to the lack of the measurement data from this site for the summer in 2008, we have adopted the measurement data in SDZ for the summer periods in 2004 (Liu et al., 2006) and in 2006 (Liu et al., 2008) as a substitute, considering the generally accepted understanding of the relatively constant feature of background concentrations within a short time peirod. Finally, we used the averaged daily profiles for July, August and September based on the 2004 and 2006 data from SDZ as the background O_3. In addition, 31 representative receptors located along the 2nd, 3rd and 4th RR and the LRs were chosen, where the hourly concentrations of CO, PM_{10}, NO_2 and O_3 were simulated for the pre-TRS, during-TRS and post-TRS periods, to evaluate the temporal and spatial variation of pollutant concentrations and air quality improvement. The road network of Beijing and the road sources of RR and LRs distributed in the study domain, including the locations of the CGZ, DL and SDZ air quality monitoring sites and the representative receptors, is shown by Fig. 1.

2.2 ADMS-Urban model set up

The ADMS-Urban model, developed by Cambridge Environmental Research Consultants (CERC, 2009), is a quasi-Gaussian dispersion model for the dispersion simulation of pollutants released from industrial, domestic and road traffic sources in urban areas. Particularly, ADMS-Urban has an advantage over other urban-scale dispersion models as it characterizes the boundary layer structure based on the Monin-Obukhov length and boundary layer height rather than the more imprecise characterization achieved with the Pasquill-Gifford stability parameter (CERC, 1999).

Various parameters which need to be set for running ADMS-Urban include surface roughness, the latitude of the modelling area, minimum Monin-Obukhov length, the chemical reaction scheme, the meteorological data and the height of recorded wind, the background data, the source data including the road width, elevation, and the canyon heights in case of modelling street canyons, the time varing factors for weekdays, Saturdays and Sundays, the road geometry indicated by the geographical coordinates of the constituting nodes, and the output parameters like the pollutants included, the number of grids for the modelling area and the heights of concentrations to be calculated for the modelling domain and the receptors, respectively.

2.2.1 Descriptive parameters and chemical reaction scheme

Descriptive parameters were used to describe the modelled area, for example, the surface roughness characterized the surrounding area in terms of the effects it would have on wind speed and turbulence, which is one of the key components of the modelling. The values chosen for some representative parameters for the modelling domain is given in Table 1.

The value of surface roughness was chosen based on some local studies (Hu, 1994; Zhang and Chen, 1997; Lu et al., 2002) and on the recommended value for modelling big cities, which is 1.0 m. The value of 30 m was chosen as the minimum Monin-Obukhov length as recommended by ADMS-Urban for cities.

ACPD
10, 5135–5184, 2010

Title Page
Abstract Introduction
Conclusions References
Tables Figures
◀◀ ▶▶
◀ ▶
Back Close
Full Screen / Esc
Printer-friendly Version
Interactive Discussion

ADMS-Urban has two chemistry options to calculate NO_2 and O_3 concentrations. The first option uses the empirical function (Derwent and Middleton, 1996). The second one is based on a chemistry scheme known as the Generic Reaction Set (GRS) (Venkatram et al., 1994), which is a semi-empirical model that simplifies photochemical reactions using a set of parameters derived from observations. The GRS scheme can work when background NO_x, NO_2 and O_3 data, as well as hourly sequential meteorological data including cloud cover are available. In ADMS-Urban, the primary NO_2/NO_x emissions fraction is assumed constant (5%) with the GRS scheme, and the NO_2 photo-dissociation coefficient is calculated using cloud cover data, in place of the radiation data. In this study, we adopted the GRS scheme to simulate the important reactions involving NO_x, VOC and O_3, since it has been demonstrated that the GRS scheme produced better results than the other option (D-M) (Vardoulakis et al., 2007).

2.2.2 Road geometry, traffic flows, fleet compositions and emission factors

The 2nd, 3rd and 4th RR, as well as the major LRs were separated into a total of 334 road segments, the lengths of which were automatically identified by Arcview, by recognizing the geographical coordinates of the road nodes constituting each segment. The width of each road segment was manually input based on field surveys. Unlike another study that focused on the traffic-related air pollution within twelve typical street canyons of Beijing using the OSPM model (Wang and Xie, 2009), this study focuses on the modelling of traffic-related air pollution around the UAB, and thus the street canyon effect was not modelled, with further consideration on the fact that the majority of roads in the UAB were not typical street canyons, of which the building heights on both sides were expected to be at least three times of the road width.

Traffic flows on each of the road segments of the 2nd, 3rd and 4th RR were intensively monitored automatically every two seconds from 10 July 2008 to 30 September 2008 by the ITS-TAP system. The high temporal resolution traffic flow data were further processed to summarize the hourly traffic flow and the hourly average running speed on each of the monitored road segments for the whole assessment period.

ACPD
10, 5135–5184, 2010

For the quality assurance and control of the traffic data, we first screened out the abnormal maximum values of monitored driving speed, replaced by the average of the normal speeds on the adjacent road segments. Moreover, the major problem of the monitored traffic flow data was the missing data on certain road segments for some periods of time. Accordingly, we treated those hourly sequential data set with a fraction of missing data over 10% by replacing them with the average of the traffic flows on the nearest upstream and downstream road segments, which had less than 10% of missing data. In addition, we eliminated the few days (6th, 13th, 14th, 24th and 28th, September) when large quantities of missing data were found. In this way, we assured that the monitored driving speed were proper, and traffic flows were relatively complete, with a possible underestimation of less than 10%.

The on-line monitored traffic flow data consisted of two vehicle categories: long vehicles which were constituted of buses and heavy duty vehicles, and short vehicles, which were constituted of passenger cars and light duty vehicles. The further split-up of the fleet on each of the road segments into these four categories were based on the surveyed fleet composition of the manual traffic counts conducted by technical assistants at the roadsides of 290 road segments in urban Beijing in 2004.

Three different sets of time-varying factors for diurnal traffic flows were identified separately for weekdays, Saturdays and Sundays, based on average traffic counts of all the road segments for each hour of the day throughout the assessment period. These profiles were used to derive time-varying emission rates (g/km/s) on all road segments for weekdays, Saturdays and Sundays, respectively, which are thought to reflect variations in diurnal emissions due to road traffic congestion or improvement in traffic conditions.

The hourly emission of CO, PM_{10}, NO_x and VOC on each road segment was calculated by using the emission factors derived from COPERT, a European emission factor model (EEA, 2000), based on the average running speed, ambient temperature and fuel property for a given vehicle category. Using the established methodology (Cai and Xie, 2007), emission factors of passenger cars, light duty vehicles, heavy duty vehicles and buses at a typical urban running speed of 20 km/h in Beijing were calculated, as shown by Table 2. Particularly, emission factors of each vehicle category on each road segment were updated in accordance with the temporal variation of running speed to improve the accuracy of source emission estimation. Together with the running speeds and the lengths of each road segment which were automatically identified by Arcview, a nested GIS (Geographical Information System) software of ADMS-Urban, the hourly emission rates of CO, PM_{10}, NO_x and VOC on each road segment were calculated.

As for ozone, a secondary air pollutant, its model-predicted concentrations over the simulated domain were based on the background measurement from SDZ background monitoring site and the results of the GRS chemical mechanism operated by ADMS-Urban, given the information of precursor pollutant emissions of NO_x and VOC.

2.2.3 Meteorological data

Transport and dispersion of air pollutants in the atmosphere are influenced by regional weather patterns. Operating on one hour intervals, meteorological data for ADMS-Urban input files include wind speed, wind direction (including anemometer height), cloud cover, precipitation and temperature, which were used by the meteorological processor of ADMS-Urban to calculate the parameters for use in the model such as boundary layer depth and Monin-Obukhov length. The complete hourly meteorological data during the assessment period were obtained from the Beijing Capital International Airport Meteorology Observatory (ZBAA), which is about 20 km northeast from the Northeast 4th RR. The daytime (8 a.m. and 2 p.m.) and nighttime (8 p.m. and 2 a.m.) wind roses during the period of 10 July–30 September 2008 are shown by Fig. 2, which reveals that northeasterly and southeasterly winds dominated in the daytime while southeasterly wind dominated in the nighttime. Consequently, the UAB was dominated by the southeasterly and northeasterly winds in the whole day during the assessment period. Besides, the majority of wind speeds during the assessment period was less than 5.0 m/s, which indicate that the dissipation of air pollutants tended to be prolonged. It was also noted that the percentage of calm wind conditions was very low (0.5%) during the assessment period, which is in favor of ADMS-Urban's performance, since modelling of traffic sources in low wind speed conditions can lead to over-predictions and is sensitive to the minimum value of wind speed used (Carruthers et al., 2000b).

2.3 Model evaluation

The evaluation of the model performance was carried out by comparing the observed hourly concentrations of CO, PM_{10}, NO_2 and O_3 at CGZ monitoring site with model predictions for the periods of 10–20 July and 10–20 August, using the statistics recommended by Hanna et al. (1991, 1993), which have been adopted as a common model evaluation framework for the European Initiative on "Harmonization within Atmospheric Dispersion Modelling for Regulatory Purposes" (Olesen, 2001). The statistical performance measures include (a) the fractional bias (FB) showing the tendency of the model to overpredict or underpredict; (b) the normalized mean square error (NMSE) showing the overall accuracy of the model; (c) the geometric mean bias (MG) showing the mean relative bias and indicating systematic errors; (d) the geometric variance (VG) showing the mean relative scatter and reflecting both systematic and random errors; (e) the Pearson correlation coefficient (R) describing the degree of association between observed concentrations and model results; and (f) the fraction of predictions within a factor of two of observations (FAC2). These statistical measures are defined as follows:

$$\mathrm{FB} = \frac{\bar{C}_o - \bar{C}_p}{0.5(\bar{C}_o + \bar{C}_p)} \quad (1)$$

$$\mathrm{NMSE} = \frac{\overline{(C_o - C_p)^2}}{\overline{C_o C_p}} \quad (2)$$

$$\mathrm{MG} = \exp(\overline{\ln C_o} - \overline{\ln C_p}) \quad (3)$$

ACPD
10, 5135–5184, 2010

A modelling study of air quality impact of odd-even day traffic restriction scheme

H. Cai and S. D. Xie

$$\mathrm{VG} = \exp\overline{[(\ln C_o - \ln C_p)^2]} \tag{4}$$

$$R = \frac{\overline{(C_o - \bar{C}_o)(C_p - \bar{C}_p)}}{\sigma_{C_p}\sigma_{C_o}} \tag{5}$$

$$\mathrm{FAC2} = \text{fraction of data that satisfy } 0.5 \le \frac{C_p}{C_o} \le 2.0 \tag{6}$$

Where: C_p are model predictions; C_o are observations; overbar($\bar{C}$) is the average over the dataset; and σ_C is the standard deviation over the dataset.

Since NMSE accounts for both systematic and random errors, it is helpful to partition NMSE into the component due to systematic errors, NMSEs, and the unsystematic component due to random errors, NMSEu. NMSEs, the minimum NMSE without any unsystematic errors, was defined by Hanna et al. (1991) for a given value of FB as:

$$\mathrm{NMSEs} = \frac{4\mathrm{FB}^2}{4 - \mathrm{FB}^2} \tag{7}$$

The above statistical measures, however, do not provide information about the model performance under diurnal variation of weather and traffic conditions. For that reason, the following qualitative performance measures have also been used: (i) diurnal pollution profiles to identify specific periods of the day when the model had good/poor performance; and (ii) pollution roses to compare predictions and observations at each of the wind directions and thus to show the model performance for different wind directions.

ACPD
10, 5135–5184, 2010

3 Results and discussion

3.1 Model evaluation

3.1.1 Overall model performance

The statistical evaluation results for CO, PM_{10}, NO_2 and O_3 based on the hourly predictions and observations are summarized in Table 3. The model predicted the concentrations of all pollutants reasonably well, with the FAC2 between 0.50 and 0.71. Besides, the FB statistic revealed that ADMS-Urban had a moderate tendency to underestimate NO_2 (FB=0.12) and O_3 (FB=0.31) concentrations, and had a moderate tendency to overestimate CO (FB=-0.22) concentrations and a slight overestimation of PM_{10} (FB=-0.0084) concentrations. The model showed satisfactory performance for NO_2 with a NMSE of 0.33, and moderate NMSE for CO, PM_{10} and O_3. Furthermore, the model performances indicated by NMSEs are very satisfactory for all pollutants, which agreed well with MG, the systematic error indicator. Besides, the model had a good performance for CO, PM_{10}, NO_2 and O_3 concentrations when considering both systematic and random errors as indicated by VG. Although the Pearson correlation coefficient for CO is relatively low (0.34), the R values for PM_{10}, NO_2 and O_3 were much higher. The R, however, is not a very robust measure due to its sensitivity to a few outlier data pairs, and thus Willmott (1982) discourages the use of R, because it does not consistently relate to the accuracy of predictions. Instead, the FAC2, which is not overly influenced by either low or high outliers, is the most robust performance measure.

A scatter plot between the observed and predicted concentrations at CGZ is presented in Fig. 3, which illustrates the robust FAC2 statistic for CO, PM_{10}, NO_2 and O_3, respectively. There was a moderate overestimation for CO probably due to the adoption of higher model-calculated emission factors, as shown by Fig. 3a, although the FAC2 for CO is high (0.71). As shown by Fig. 3b, predicted and observed PM_{10} concentrations agreed very well with each other, with its scatter plot almost symmet-

ACPD
10, 5135–5184, 2010

rical. Figure 3c reveals that a majority (69%) of predicted concentrations fall within a factor of two of the observations for NO_2, with a slight underestimation. The higher NO_2 observations might derive from the enhanced photochemical reactions of NO with oxidants such as peroxy radicals that were present either in the atmosphere or in vehicle exhaust (Kenty et al., 2007). Ozone was moderately underestimated, as revealed by Fig. 3d, but was still satisfactorily predicted when taking into account the limitation of the simplified GRS scheme adopted in predicting secondary pollutant like ozone.

3.1.2 Dependence of model performance on time-of-the-day

Diurnal profiles on hourly average have been separately plotted for all pollutants measured and predicted at CGZ, as shown by Fig. 4. The model captured well the diurnal variations of CO, PM_{10}, NO_2 and O_3, and did particularly well for NO_2 and O_3 at predicting the observed peaks. The predicted morning peaks of CO and PM_{10} were about three hours earlier than the observed, but were in good agreement with the morning peak of traffic flows. In addition, the temporal variations of predicted CO and PM_{10} concentrations changed more dramatically than the observed, with a notably overprediction in peak CO concentrations, which was mainly related to an overestimation of the CO emission factor adopted by the model, resulting in a relatively larger overestimation of emission rates during the rush hours with higher traffic flows than other periods of the day. Moreover, Fig. 4 showed that the model had an excellent performance in predicting the diurnal profile of NO_2 and O_3, which revealed the satisfactory model performance in reasonably predicting the temporal variation of secondary gases like NO_2 and O_3 with the application of the GRS chemical scheme. Consequently, the model captured the evening peak NO_2 concentrations, and the afternoon peak ozone concentrations accompanied by the trough NO_2 concentrations.

3.1.3 Dependence of model performance on wind direction

Although wind speed has an important influence on the dispersion of pollutant and thus the model predictions of pollutant concentrations, we do not focus on the evaluation of the dependence of model performance on wind speed, because the fundamental factor influencing the diurnal profile of model predictions was the temporal variation of source intensity and subsequent atmospheric chemical reactions, rather than the accompanying wind speed. However, to evaluate the dependence of model performance on wind direction was important to know whether the meteorological station adopted in this study was representative of the wind field of the study domain, and to understand for the right reason the characteristics of spatial distribution of the traffic-related air pollution after the TRS was implemented. Thus, the pollution roses for all pollutants were plotted, as shown by Fig. 5, which revealed that the peaks and troughs of the predicted and observed concentrations were virtually in the same directions. This proved that the model well predicted the variance of concentrations in response to the wind direction variation. Besides, Fig. 5 also revealed that there was a clear dependence of concentrations on wind directions for all pollutants: high CO concentrations occurred mainly in the downwind southwesterly, northwesterly and southerly directions, with high PM_{10} concentrations also occurring in the downwind southwesterly and northwesterly directions. In addition, NO_2 concentration had a weaker dependence on wind directions and distributed more uniformly in each direction, with the peak concentrations mainly occurring in the southwesterly direction. O_3 had a very clear dependence of wind direction, with the peak concentrations appearing in the northwesterly and southwesterly directions. Therefore, the model captured well the spatial variation of the pollutant concentrations in response to the wind direction variation, which revealed that the meteorological data from the Airport Meteorological Observatory were well representative of the wind field of UAB, in consistence with another study using the same meteorological data source for the evaluation of air quality impacts of the Games (Wang et al., 2009a).

3.2 Air quality impacts in response to TRS policy before, during and after the Games

Applying the evaluated ADMS model, we predicted the CO, PM_{10}, NO_2 and O_3 concentrations from the RRs and LRs around UAB before, during and after the Olympic Games, with the aim of evaluating the air quality impacts of the TRS policy. First, the emission reduction in accordance with the decrease of traffic flows was reported; Second, the daily and diurnal variation of pollutant concentrations along the RRs and LRs were compared for the pre-, during- and post-TRS periods, followed by a further assessment of the weekly variation of air quality in response to the TRS policy; Finally, the spatial variation of the traffic-related air pollution for the pre-, during- and post-TRS periods was assessed, to understand the regional differences in air quality impacts of the TRS policy.

3.2.1 Reduction of diurnal average traffic flow and pollutant emissions

The traffic flows on the RRs and LRs had a notable reduction after the TRS policy was implemented on 20 July 2008. The daily average traffic flows of the short and long motor vehicles for the during-TRS period had a reduction of 26.1% and 11.0%, respectively, compared to the pre-TRS period. Figure 6, which shows the variation of traffic flows on RRs and LRs on daily average and the variation of the diurnal profiles of the total traffic flow on hourly average for the pre-TRS, during-TRS and post-TRS periods, revealed that the TRS policy had a substantial effect on the reduction of both daily average and hourly average traffic flows, with average reduction rates of 22.4%, 26.1%, 27.7% and 27.6% on the 2nd, 3rd, 4th RR and the LRs, respectively, and a notably overall reduction of about 26.1% for the total traffic flow. Particularly, the TRS policy had a largest traffic flow reduction of 30.8% during the morning rush hours (7–8 a.m.). On the other hand, both the daily average and hourly average traffic flows on all types of roads during the post-TRS period virtually bounced to the same level as the pre-TRS period, with the double-peak pattern of the diurnal profile of traffic flows in

ACPD
10, 5135–5184, 2010

Beijing unchanged by the TRS policy.

With the reduction of traffic flows, the traffic conditions were improved and the traffic running speeds on hourly average increased by about 15% for the during-TRS period, as revealed by the ITS-TAP monitoring network. The raised speed decreased the emission factors of CO, PM_{10} and NO_x for all vehicle types, as calculated by COPERT model. In addition to the reductions of traffic flows and emission factors, the emissions on daily average decreased by about 26.1%, 25.4% and 25.2% for CO, PM_{10} and NO_x, respectively. Consequently, emission rates on the RRs and LRs decreased as well, especially for the 3rd, 4th RR and the LRs.

3.2.2 Temporal variation of air quality impacts of the TRS policy

Pollutant concentration levels were directly related to air quality, and thus we focused on the pollutant concentration impacts of the TRS policy to assess its effectiveness on air quality improvement in Beijing during the Games. Concentrations of CO, PM_{10}, NO_2 and O_3 in the following results and discussion were predicted at a height of 1.5 m above the ground.

Changes in daily average concentrations for the pre-, during- and post-TRS periods

The daily average concentrations of CO, PM_{10}, NO_2 and O_3 had a notable reduction on the RRs and LRs around UAB after the TRS policy was implemented, as shown by Fig. 7, which illustrates that the daily average predictions of CO, PM_{10}, NO_2 and O_3 on the 2nd, 3rd, 4th RR and the LRs for the pre-, during- and post-TRS periods. Daily average CO concentrations were about 2.1, 2.1, 2.2 and 2.3 mg/m^3 on the 2nd, 3rd, 4th RR and LRs, respectively, for the pre-TRS period, which decreased by about 35.8%, 38.5%, 34.9% and 35.6% on the 2nd, 3rd, 4th RR and LRs, respectively, for the during-TRS period. Consequently, the CO daily concentrations on all road types satisfied the CNAAQS Grade II of 4 mg/m^3 for the during-TRS period. The pre-TRS daily average concentrations of PM_{10} were 120.9, 115.7, 136.1 and 163.2 μg/m^3 on the 2nd, 3rd, 4th RR and the LRs, respectively, which were successfully reduced below the daily CNAAQS Grade II of 150 μg/m^3 by the TRS policy, as shown by Fig. 7. For the pre-TRS period, 40% of days on the LRs exceeded 150 μg/m^3, while the PM_{10} daily concentrations on the LRs were successfully reduced by 34.7%, to satisfy the Grade II limit, with the PM_{10} concentrations on the 2nd, 3rd and 4th RR reduced by 38.7%, 31.8% and 44.0%, respectively, resulting in satisfaction of the Grade II limit for every single day for the during-TRS period. With the bounce of traffic flows during the post-TRS period, concentrations of both CO and PM_{10} increased notably, with 20% of days on the LRs exceeds the Grade II limit for PM_{10}. The NO_2concentrations were reduced by about 30.3%, 31.9%, 32.3% and 33.9% on the 2nd, 3rd, 4th RR and the LRs, respectively, to about 52.3, 46.2, 45.9 and 47.0 μg/m^3 during the TRS period, with the daily concentration on every single day during this period conforming to the CNAAQS Grade II of 80 μg/m^3. Only 10% of days on the 2nd RR exceeded the NO_2 Grade II limit for the post-TRS period, despite a concentration increase of about 9.0%, 13.7%, 17.3% and 18.8% on the 2nd, 3rd, 4th RR and the LRs, respectively, during the period. O_3, of which the concentration level is usually lower in the source-intensive urban areas than in the rural areas, had a concentration of about 38–52 μg/m^3 in the urban areas during the pre-TRS period, and the O_3 concentration decreased to about 24-29 μg/m^3 during the TRS period, which was consistent with the findings of Wang et al. (2009b). Unlike other pollutants, the O_3 concentration continued decreasing for the post-TRS period, to about 23–26 μg/m^3 despite the increase of traffic flow and vehicular emissions. This is mainly because O_3 concentrations in UAB are produced by local photochemical reactions under VOC-limited conditions (Wang and Li, 2002; Wang et al., 2009), and higher emission level of NO during the post-TRS period consumed O_3 and suppressed the accumulation of O_3 in urban environment of Beijing (named the "titration effect") (Chou et al., 2006; Sadanaga et al., 2008). Besides, the elevated nitrogen dioxide (NO_2) through the titration effect and reactions of NO with other radicals further reacted with the OH radical and yielded nitric acid (HNO_3), which ended the photochemical reaction chain involved with the OH radical that otherwise accumulates the ambient O_3 concentration (NARSTO, 2000). Therefore, it was clear that the TRS policy was effective in reducing daily average concentrations of pollutants, ensuring that the air quality in Beijing during the Olympic Games conforming to the 24 h CNAAQS Grade II limits.

The predicted highest daily average concentrations of the CO, PM_{10}, NO_2 and O_3, which occurred at a very limited area under certain circumstances, also showed a notable decrease during the TRS period, which was in consistent with the previous study proving the effectiveness in reducing extreme concentrations of a four-day traffic control experiment by the Beijing Municipal Government (Westerdahl et al., 2009). The predicted highest concentrations had decreased from 6.3 to 4.6 mg/m^3 for CO, from 635.7 to 498.3 µg/m^3 for PM_{10}, from 194.7 to 154.2 µg/m^3 for NO_2 and from 88.2 to 53.3 µg/m^3 for O_3, a reduction of about 27.6%, 21.6%, 20.8% and 39.6% for CO, PM_{10}, NO_2 and O_3, respectively, in comparison with the pre-TRS period.

Diurnal variation of hourly average concentration

To further evaluate the effectiveness of the TRS policy on air quality improvement, we focused on the variation of diurnal profiles of hourly average concentration on the RRs and LRs in response to the TRS policy. Figure 8 shows that hourly average concentrations of CO, PM_{10}, NO_2 and O_3 on the RRs and the LRs decreased notably, in comparison with the pre-TRS period. The morning and evening peak concentrations of CO on the LRs had decreased from about 3.29 mg/m^3 to about 1.83 mg/m^3, the largest reduction of 34.9% and 38.0% among all road types, as shown by Fig. 8a, while the largest reduction of the morning and evening peak concentrations of PM_{10} was observed on the 2nd RR, accounting for about 37.8% and 40.2%, respectively. Consequently, the hourly CO concentrations were well below the 1-hour CNAAQS Grade II of 10 mg/m^3 and the hourly PM_{10} concentrations decreased below 150 µg/m^3 on all types of roads. Particularly, the average of evening peak CO, PM_{10} and NO_2 concentrations were reduced significantly, by about 36.6%, 36.1% and 32.8%, respectively, which was a solid

ACPD
10, 5135–5184, 2010

A modelling study of air quality impact of odd-even day traffic restriction scheme

H. Cai and S. D. Xie

proof for the air quality improvement during the TRS policy period.

For both pre- and during-TRS periods, the diurnal profile of CO and PM_{10} took on an obvious double-peak mode, as shown by Fig. 8a and b, with the morning and evening peak concentrations occurring at around 7–8 a.m. and around 8–9 p.m., respectively, and the lowest concentrations occurring at around 3 am. While the occurring time of the morning peak concentration was consistent with the morning rush hour of traffic flows, the evening peaks for CO and PM_{10} were about two to three hours later than the evening rush hour. Moreover, the evening peak concentrations of CO and PM_{10} during the pre-TRS period even exceeded the morning peak, which was in contradiction with the diurnal profile of traffic flows during the period. These delayed and higher evening peak concentrations should be ascribed to the particular evening meteorological conditions in UAB: urban heat island (UHI) frequently occurs in Beijing in the summer night, which tends to produce strong temperature inversion and higher inversion layer at night. When the UHI occurred, the UHI convergence and the strong temperature inversion at night hindered air dispersion and contributed to the local accumulation of pollutants, resulting in high pollution concentrations at night (Miao et al., 2008; Liu et al., 2006).

The NO_2 concentrations on all roads for the pre-TRS periods, as shown by Fig. 8c, began to increase in the early morning, reached a peak at about 7–8 a.m., and came to a trough during the mid-day time, which was related to the traffic and emission rate cycles and similar diurnal variation of NO_2 concentrations were found in the urban area of Cairo (Khoder, 2009). The maximum concentration of NO_2 occurred at about 7–8 p.m., which was higher in magnitude than the morning peak. This was partly due to the evening rush hour of traffic with high emission rate of NO_x, and partly due to the same UHI effect weakening the dispersion conditions and resulting in evening peak concentrations of CO and PM_{10}. Moreover, the lower temperature and solar radiation intensity in the evening decreased the photodissociation of NO_2, a major chemical mechanism for NO_2 loss during the daytime. The TRS policy, as shown by Fig. 8c, did not alter the diurnal variation characteristic of NO_2 concentrations, but significantly

ACPD
10, 5135–5184, 2010

reduced the hourly sequential concentrations of NO_2 during the Games. Particularly, the highest hourly average concentrations of 123.1, 107.2, 111.9 and 116.6 μg/m^3 on the 2nd, 3rd, 4th RR and the LRs, respectively, which occurred at about 7 p.m. during the pre-TRS period, were significantly reduced by as much as 38.6%, 31.5%, 34.7% and 32.5%, respectively, to 77.5, 73.4, 73.1 and 75.7 μg/m^3, respectively, during the TRS period, which was in good agreement with the tropospheric NO_2 observations by NASA's OMI revealing a 30–50% reduction of NO_2 during the Games (NASA, 2009). Therefore, the TRS policy was effective in reducing the hourly NO_2 concentrations, and consequently the hourly concentrations on all types of roads were far below the 1-h CNAAQS Grade II of 120 μg/m^3 during the TRS period. As shown by Fig. 8d, the O_3 concentrations on all roads had a similar diurnal profile for both pre- and during-TRS periods, with the concentrations increasing in the daytime, reaching the peak at about 3 p.m. and beginning to decrease rapidly. It was clear that the TRS policy reduced remarkably the hourly O_3 concentrations on all types of roads, and had a notable concentration reduction of the afternoon peak, with the concentrations on the 2nd, 3rd, 4th RR and the LRs decreasing by about 35.4%, 30.7%, 32.2% and 31.8%, respectively. As a result, the hourly O_3 concentration during the TRS period was far below the 1-h CNAAQS Grade II of 160 μg/m^3. Meanwhile, it was interesting to find that the diurnal variation of the concentration ratio of NO_2 to O_3 ([NO_2]/[O_3]) for all types of roads was opposite to the diurnal profile of O_3 concentrations, which revealed that the traffic-related NO_x (mostly NO) consumed O_3, and resulted in an increase of the secondary NO_2 concentration and a decrease of the O_3 concentration, a typical VOC-limited characteristic for ozone formation. With the significant reduction of both primary and secondary pollutant concentration levels, air quality in UAB had therefore been improved remarkably during the Games in response to the TRS policy.

Weekly variation of diurnal profile of pollutant concentrations for the pre-, during- and post-TRS periods

To investigate the day-of-the-week variation of air quality impact in response to the TRS policy, we plotted the diurnal profiles of CO, PM_{10}, NO_2 and O_3 for weekdays, Saturdays and Sundays for the separate periods before, during and after the TRS policy. As shown by Fig. 9a and b, the diurnal profiles for CO and PM_{10} remained similar, with a typical two-peak pattern, and had no obvious weekly variation in response to the TRS policy, as the occurring time of the peaks and trough were consistent for weekdays, Saturdays and Sundays for the three separate periods, due to the smooth weekly cycle of diurnal variation of traffic flows. Notably lower levels of CO and PM_{10} concentrations on Saturdays and Sundays than weekdays, however, were observed, particularly during the rush hours when peak concentrations occurred, for the pre-, during- and post-TRS periods. Therefore, it was clear that the traffic-related air pollution still presented a typical two-peak diurnal variation pattern, but the weekly cycle had no obvious variation in response to the TRS policy, which was, nevertheless, effective in reducing the hourly concentrations, particularly the peak concentrations of CO and PM_{10}.

The day-of-the-week variation of NO_2 diurnal profile, as shown by Fig. 9c, revealed a similarity in the diurnal variation on weekdays, Saturdays and Sundays, particularly, in the ascending trend of NO_2 concentrations in the daytime and reaching a peak in the evening, despite a notable decrease in the afternoon, for the pre-, during- and post-TRS periods. Besides, lower concentration levels on Saturdays and Sundays were observed compared to that on weekdays, which revealed that the TRS policy did not change the weekly cycle of traffic flows, with heavier traffic load on weekdays than on the weekends. Meanwhile, Fig. 9d revealed a notable difference between the diurnal profile of O_3 and other pollutants, with relatively higher concentration levels on Saturdays and Sundays than that on weekdays for the pre- and post-TRS periods, which was in agreement with the characteristic of the ozone weekend effect that has been frequently observed in urban areas (Atkinson-Palombo et al., 2006; Gao and Niemeier,

ACPD
10, 5135–5184, 2010

A modelling study of air quality impact of odd-even day traffic restriction scheme

H. Cai and S. D. Xie

2007; Murphy et al., 2007; Tang et al., 2008; Khoder, 2009). The major reason for the observed ozone weekend effect was the "VOC-limited" feature for ozone formation in UAB: the ozone concentration tended to increase with the decrease of NO_x emissions, typically due to the reduction of traffic flows, as a result of the weakened titration effect of lower NO_x emissions on the weekends that tended to accumulate ozone concentrations. This mechanism also explained why a more remarkable ozone weekend effect was observed for the post-TRS period, as shown by Fig. 9d: the peak O_3 concentration at around 3 p.m. on weekdays for the post-TRS period continued to decrease, compared to the during-TRS period, due to the enhanced titration effect of increased NO_x emissions that suppressed the ozone formation on weekdays, while the peak concentrations on Saturdays and Sundays increased, due to a larger reduction of NO_x emissions and thus a more weakened titration effect on the weekends during the post-TRS period, compared to the during-TRS period. Moreover, Fig. 9d also revealed that the TRS policy effectively reduced both the hourly peak and daily average concentrations of ozone, and meanwhile reduced and virtually removed the weekend effect of ozone for the during-TRS period, probably due to the smoother weekly variation of traffic flows resulting from the restriction on traffic.

3.2.3 Spatial variation of traffic-related air pollution and implication on regional air quality improvement for the pre-, during- and post-TRS periods

To investigate the regional air quality impacts of the TRS policy, we looked into the spatial distribution of the traffic-related air pollution around UAB, as well as the spatial variation of regional air quality improvement in response to the TRS policy. Figure 10, which illustrates the contour plot of the daily average concentrations of CO, PM_{10}, NO_2 and O_3 from on-road motor vehicles on the 2nd, 3rd, 4th RR and the LRs, for the pre-, during- and post-TRS periods, respectively, revealed remarkable differences in the regional distribution of traffic-related air pollutant concentrations and notable variation of regional air quality in response to the TRS policy. Before the TRS policy was placed, the highest and lowest CO concentration levels occurred in the upwind eastern regions

ACPD
10, 5135–5184, 2010

H. Cai and S. D. Xie

and the southern areas, respectively, as shown by Fig. 10a, with the daily average concentrations of the representative receptors located in the downwind northwest and upwind southeast accounting for about 2.56 and 2.02 mg/m^3, respectively. Particularly, the West 2nd RR and the Northwestern LRs between 2nd, 3rd and 4th RR had the heaviest traffic and accordingly suffered the highest CO concentration level of above 2.4 mg/m^3. With the TRS policy, a significant reduction of the CO daily average concentration was achieved, and the previously highest concentration in the north was reduced by 31.2%, to 1.79 mg/m^3, with the concentration levels in the south, west and east regions decreasing by about 17.6%, 18.2% and 17.6%, respectively. Besides, CO concentrations in a broad area of the northeast, east and southeast outside the 4th RR decreased below a level of 0.5 mg/m^3, mainly due to the prevailing northeast, east and southeast wind that transported the pollutant to the downwind directions and resulted in a relatively lower concentrations in these upwind areas during the period. Moreover, the previously seriously polluted areas in the West 2nd RR and the Northwestern LRs were relieved, with a much smaller area where the concentration level remained above 2 mg/m^3. Therefore, the TRS policy was effective in bringing down the concentration levels in both the most polluted areas and different parts of the urban area, resulting in a much better air quality during the Games. With the bouncing of traffic flows almost to the pre-TRS level, the CO concentration increased dramatically in every part of UAB, and consequently, almost caught up with the previous level before the TRS policy was placed, with the concentrations in the east, south, west and north increasing by about 24.2%, 16.0%, 15.2% and 22.2%, respectively.

The spatial distribution of PM_{10} concentrations was characterized as linear distribution of relatively higher pollution along the RR and the LRs, with concentration levels in the areas between the monitored roads and outside the 4th RR much lower. For the during-TRS period, the PM_{10} concentration levels decreased remarkably for the whole UAB, with the PM_{10} concentration in most of the area reduced below 100 µg/m^3. Particularly, the previously highly polluted areas in the West 2nd RR, Southwestern 4th RR and the Northern LRs with PM_{10} concentrations above 150 µg/m^3 before the TRS shrank significantly during the TRS, as shown by Fig. 10b. Consequently, the concentrations in the east, south, west and north regions of UAB decreased from about 118.2, 111.9, 160.4 and 217.7 μg/m^3, respectively, for the pre-TRS period, to about 66.1, 67.6, 105.6 and 155.2 μg/m^3, respectively, for the during-TRS period. The dramatical decrease of the primary pollutant concentration indicated that the air quality during the Games was improved significant in response to the TRS policy. However, the PM_{10} concentration levels increased by about 23.4%, 33.6%, 20.7% and 29.5%, respectively, in the east, south, west and north regions for the post-TRS period. As a result, the areas with PM_{10} concentration above 150 μg/m^3 expanded, which proved reversely the effectiveness of the TRS policy on air quality improvement.

The spatial distribution of NO_2 concentration was more influenced by the prevailing northeasterly, easterly and southeasterly winds during the pre-TRS period, with the relatively higher daily average concentration of about 76.8 and 68.0 μg/m^3 predicted in the downwind western areas and the northern traffic-heavy areas, respectively. Besides, the daily average NO_2 concentration along the West 2nd RR, the Northern LRs and part of the West 4th RR exceeded the CNAAQS Grade II of 80 μg/m^3. On the contrast, the NO_2 concentration decreased significantly in response to the TRS period, with the concentration level in most of UAB below 80 μg/m^3, which was a clear evidence of the effective control of traffic-related air pollution and corresponding remarkable air quality improvement by the TRS policy. Particularly, better effect on pollution reduction was observed in the previously most severely polluted areas, as the concentration levels in these areas were brought down sufficiently to comply with the CNAAQS limited values. With the expiration of the TRS policy, NO_2 pollution with concentration above 80 and even 120 μg/m^3 appeared in a much larger area for the post-TRS period, and NO_2 concentration increased significantly in the downwind western areas, in comparison with the during-TRS period, as shown by Fig. 10c. The spatial distribution variation of NO_2 concentration in UAB revealed a notable air quality improvement due to reduced on-road vehicular emissions.

The spatial distribution of O_3 concentration was distinct from those of CO, PM_{10} and

ACPD
10, 5135–5184, 2010

NO_2, as shown by Fig. 10d. For the pre-, during- and post-TRS periods, notably lower O_3 concentrations were observed along the RR and the LRs as these areas were the emission sources and O_3, as a typical secondary air pollutant, had its higher concentration levels in the relatively remote areas off the road sources. Consequently, the O_3 daily average concentration in the near-road areas was well below 60 µg/m^3 for the pre-TRS period and relatively higher concentration levels of 60–80 µg/m^3 and above 80 µg/m^3 covered a large area around and outside UAB where no direct vehicular emissions were generated. Particularly, the severely polluted West 2nd RR, Northern LRs and part of the South 4th RR areas with high concentration levels of CO, PM_{10} and NO_2, however, had the lowest O_3 concentrations. In response to the TRS policy, the O_3 concentrations in the East, South, West and North regions of UAB decreased significantly from 43.3, 46.6, 36.4 and 43.9 µg/m^3, respectively, to about 30.7, 31.2, 23.7 and 24.4 µg/m^3, respectively, mostly due to the decrease of the precursor emissions of NO_x and VOC from on-road vehicles. Moreover, the O_3 concentration during the post-TRS period continued to decrease, despite the increase of vehicular emissions of NO_x and VOC. As has been discussed previously, this phenomenon was mostly due to the "VOC-limited" characteristic for ozone formation in UAB. Therefore, the spatial variation of O_3 concentrations in response to the TRS policy also provided solid evidence of the effectiveness of such a restriction policy on air quality improvement during the Games.

3.3 Contribution of traffic flow reduction, raise of running speed and meteorological conditions to air quality improvements during the TRS period

It is meaningful to understand deeply the reasons that resulted in the air quality improvement after the TRS policy was implemented, to make sure that the model performed well for the right reasons, and to learn and inherit the useful experiences for the future air quality management in Beijing and other cities of China. Therefore, we focused on a discussion about the air quality impacts of traffic flow reduction, raise of running speed, variation of emission factors of pollutants, as well as the meteorological condition variation during the Games.

The TRS policy had a direct impact on the traffic flow and the running speeds of traffic fleet. As revealed by the ITS-TAP system, the daily average traffic flows of short and long vehicles during the TRS period decreased by 26.1% and 11.0%, respectively, an average reduction of about 24.2% for the total traffic fleet, in comparison with the pre-TRS period. Besides, running speed on the 2nd, 3rd, 4th RR and the LRs increased by 18.5%, 12.8%, 15.3% and 13.8%, respectively, an average 15% increase in driving speeds of total traffic fleet, estimated based on the fractions of traffic flows on these roads after the TRS policy took effect, which had a positive effect on reducing emission factors of pollutants. Figure 11a illustrates the decrease rates of model-calculated emission factors of CO, PM_{10} and NO_x from various vehicle types resulting from the raise of running speed. The PC and LDV, which were mostly gasoline vehicles, had the largest reduction of CO emission factor, accounting for about 10%. The largest reductions of both NO_x and PM_{10} emission factors were ascribed to diesel HDV, of which the traffic flow accounted for only 1–2% of the total fleet. Therefore, the reduction of NO_x emission factor mainly relied on the other vehicle types, and an overall 3% reduction in NO_x emission factor was achieved. The PM_{10} emission factors were assumed constant for gasoline PC and LDV in response to the running speed increase, as there were no domestic studies available reporting the variation of PM emission factors of gasoline vehicles induced by speed raise, like from 20 km/h to 23 km/h, and a comprehensive sensitivity evaluation of the USEPA's MOBILE 6.2 model for PM emission factor found that a speed increase from 20 km/h to 23 km/h had very little impact on PM emission factor and concluded that speed has a negligible effect on PM emission factors for gasoline vehicles, which was unlike the emission factors for CO NO_x and VOC that were highly sensitive to speed (Granell et al., 2004), while the HDV and buses had a reduction of about 10% of PM_{10} emission factor. Consequently, the emissions of CO, PM_{10} and NO_x were reduced by about 26.1%, 25.4% and 25.2%, respectively, and the daily average concentrations of CO, PM_{10}, NO_2 and O_3 decreased by about 25.5%, 35.4%, 32.1% and 34.4%, respectively, in response to the TRS policy. Therefore, the

TRS policy was effective in bringing down traffic-related emissions, by a dominant contribution of traffic flow reduction, and by an extra bonus of decreasing emission factors due to the improvement of driving conditions. Taking into account the variation of wind speed, a major meteorological factor that affected the traffic-related air pollution, the daily average wind speeds were about 2.52 and 2.53 m/s for the pre- and during-TRS periods, respectively, and had no statistically significant difference ($p<0.05$). Besides, the diurnal wind speed profile on the hourly average had little variation, particularly in the morning and for the evening rush hours (7–8 p.m.), as shown by Fig. 11b. Under the virtually constant wind speed, the TRS policy turned out an effective measure in simultaneously bringing down traffic flow, increasing traffic fluency, and achieving air quality improvement with significantly decreased concentration levels. Therefore, the TRS policy was effective in reducing short-term traffic-related air pollution and improving air quality promptly, which could be considered as a feasible alternative in pollution control and air quality assurance in megacities of China like Beijing under particular or emergency occasions.

4 Conclusions

We conducted a modelling evaluation of the air quality impacts of the odd-even day traffic restriction scheme implemented by the Beijing Municipal Government during the 2008 Olympic Games, and proved that this policy was effective in reducing short-term traffic-related air pollution and substantially improved the air quality in the urban area of Beijing during the Games.

The ADMS-Urban was well evaluated with hourly observations from an air quality monitoring station, and produced satisfactory predictions, based on the high temporal resolution on-road traffic flow data retrieved from the ITS-TAP monitoring network covering the 2nd, 3rd, 4th RR and the LRs distributing over the major UAB, and on the hourly meteorological data from a representative Observatory. This study demonstrated that modelling-based air quality evaluation was a reliable approach and was especially useful for simultaneous and intensive assessment of air quality responses at multi-receptor and in different regions of the study domain.

Both daily average and maximum concentrations of CO, PM_{10}, NO_2 and O_3 during the pre-TRS period deceased significantly to much lower levels during the TRS period, with the daily average concentrations from on-road vehicles conforming to the CNAAQS Grade II. However, pollutant concentrations of CO, PM_{10} and NO_2 increased for the post-TRS period, with the exception for O_3 concentration, which continued decreasing, mainly due to the "VOC-limited" characteristic for ozone formation in UAB. The bouncing of pollutant concentration levels of CO, PM_{10} and NO_2 after the expiration of the TRS policy just reversely reflected the effectiveness of the TRS in improving short-term air quality.

The hourly average, especially the peak concentrations of CO, PM_{10}, NO_2 and O_3 were reduced significantly in response to the TRS policy. However, the TRS policy did not change the typical two-peak diurnal variation pattern of the primary pollutants (CO and PM_{10}). Besides, no remarkable weekly variation of pollutant concentrations were revealed as a result of the TRS policy, with the concentration levels of CO, PM_{10}, NO_2 on weekday generally higher than those on weekends. Particularly, a notable ozone weekend effect with higher concentrations on weekends was revealed, mostly due to the decreased NO_x emissions on weekends and the "VOC-limited" characteristic for ozone formation in UAB. Meanwhile, a remarkable reduction of peak hour and daily average concentrations of O_3 was achieved in response to the TRS policy.

Notable air quality improvement was revealed around UAB during the Games, which indicated the overall effectiveness of the TRS policy. Particularly, better effect on pollution reduction was observed in the previously most severely polluted areas, where the concentration level decreased sufficiently to comply with the CNAAQS guidelines. Besides, significant air quality improvement was achieved in the upwind eastern and southern areas in response to the TRS policy. In conclusion, the TRS policy was effective in significantly improving short-term and regional air quality in UAB during the Games, and provided valuable experiences for future temporary and regional control of traffic-related air pollution.

Acknowledgements. This work was supported by the financial support from the Research on Optimizing the Stationing of Monitoring Sites for Urban Ambient Air Quality (No. 200709001), from the Research on Photochemical Smog Pollution and Public Prewarning Standards in Key Cities (No. 200800034), from Shanghai Tongji Gao Ting-yao Environmental Science and Technology Development Foundation, and from the Doctoral Thesis Scholarship of China Development Research Foundation funded by General Motors.

References

Assael, M. J., Delaki, M., and Kakosimos, K. E.: Applying the OSPM model to the calculation of PM_{10} concentration levels in the historical centre of the city of Thessaloniki, Atmos. Environ., 42, 65–77, 2008.

Atkinson-Palombo, C. M., Miller, J. A., and Balling, R. C.: Quantifying the ozone "weekend effect" at various locations in Phoenix, Arizona, Atmos. Environ., 40, 7644–7658, 2006.

Beijing Municipal Environmental Protection Bureau: Beijing Environmental Bulletin, http://www.bjepb.gov.cn, 2009.

Bennett, M. and Hunter, G. C.: Some comparisons of lidar estimates of peak ground-level concentrations with the predictions of UK-ADMS, Atmos. Environ., 31, 429–439, 1997.

Berkowicz, R.: OSPM – a parameterised street pollution model, Environ. Monit. Assess., 65, 323–331, 2000.

Berkowicz, R., Ketzel, M., Jensen, S. S., Hvidberg, M., and Raaschou-Nielsen, O.: Evaluation and application of OSPM for traffic pollution assessment for a large number of street locations, Environ. Modell. Softw., 23, 296–303, 2008.

Cai, H. and Xie, S. D.: Estimation of vehicular emission inventories in China from 1980 to 2005, Atmos. Environ., 41, 8963–8979, 2007.

Cai, H. and Xie, S. D.: Tempo-spatial variation of emission inventories of speciated volatile organic compounds from on-road vehicles in China, Atmos. Chem. Phys., 9, 6983–7002, 2009,
http://www.atmos-chem-phys.net/9/6983/2009/.

Cambridge Environmental Research Consultants (CERC): http://www.cerc.co.uk/environmental-software/ADMS-Urban-model, Cambridge, UK, 2009.

Carruthers, D. J., Holroy, D. R. J., Hunt, J. C. R., Weng, W. S., Robins, A. G., Apsley, D. D., Thomson, D. J., and Smith, F. B.: UK-ADMS – a new approach to modeling dispersion in the earth's atmospheric boundary-layer, J. Wind. Eng. Ind. Aerod., 52, 139–153, 1994.

Carruthers, D. J., Mckeown, A. M., Hall, D. J., and Porter, S.: Validation of ADMS against wind tunnel data of dispersion from chemical warehouse fires, Atmos. Environ., 33, 1937–1953, 1999.

Carruthers, D. J., Dyster, S., and McHugh, C. A.: Contrasting methods for validating ADMS using the Indianapolis dataset, Int. J. Environ. Pollut., 14, 115–121, 2000a.

Carruthers, D. J., Edmunds, H. A., Lester, A. E., McHugh, C. A., and Singles, R. J.: Use and validation of ADMS-Urban in contrasting urban and industrial locations, Int. J. Environ. Pollut., 14, 364–374, 2000b.

Carruthers, D. J., Dickson, P., McHugh, C. A., Nixon, S. G., and Oates, W.: Determination of compliance with UK and EU air quality objectives from high-resolution pollutant concentration maps calculated using ADMS-Urban, Int. J. Environ. Pollut., 16, 460–471, 2001.

Cambridge Environmental Research Consultants (CERC): ADMS-Urban User Guide 2.2, http://www.cerc.co.uk/environmental-software/assets/data/doc_userguides/CERC_ADMS_Urban2.2_User_Guide.pdf, Cambridge, UK, 1999.

Chan, C. K. and Yao, X.: Air pollution in mega cities in China, Atmos. Environ., 42, 1–42, 2008.

Cheng, Y. F., Heintzenberg, J., Wehner, B., Wu, Z. J., Su, H., Hu, M., and Mao, J. T.: Traffic restrictions in Beijing during the Sino-African Summit 2006: aerosol size distribution and visibility compared to long-term in situ observations, Atmos. Chem. Phys., 8, 7583–7594, 2008, http://www.atmos-chem-phys.net/8/7583/2008/.

Chinese Olympic Committee: The temporary traffic control implementations for non-Beijing local vehicles during 2008 Beijing Olympic and Paralympic Games, http://www.beijing2008.cn/news/olympiccities/beijing/n214412173.shtml, 20 June, 2008.

Chou, C. C. K., Liu, S. C., Lin, C. Y., Shiu, C. J., and Chang, K. H.: The trend of surface ozone in Taipei, Taiwan, and its causes: Implications for ozone control strategies, Atmos. Environ., 40, 3898–3908, 2006.

Derwent, R. G. and Middleton, D.R.: An empirical function for the ratio NO_2/NO_x, Clean Air (NSCA), 26, 57–60, 1996.

Elbir, T.: Application of an ISCST3 model for predicting urban air pollution in the Izmir metropolitan area, Int. J. Environ. Pollut., 18, 498–507, 2002.

European Environment Agency: COPERT III-Computer programme to calculate emissions from road transport, methodology and emission factors (version 2.1), technical report No. 49, 5–6, 2000.

European Space Agency and Minister of Science and Technology, China: BeijingAir, street-scale air pollution forecasts for Beijing, http://www.beijingairquality.cn, 2008.

Fang, M., Chan, C. K., and Yao, X. H.: Managing air quality in a rapidly developing nation: China, Atmos. Environ., 43, 79–86, 2009.

Gao, H. O., and Niemeier, D. A.: The impact of rush hour traffic and mix on the ozone weekend effect in southern California, Transport. Res. D-Tr. E., 12, 83-98, 2007.

Granell, J., Ho, C., Tang, T., and Roberts, M.: Analysis of MOBILE6.2's PM emission factor estimating function, USEPA's 13th International Emission Inventory Conference "Working for Clean Air in Clearwater", http://www.epa.gov/ttn/chief/conference/ei13/mobile/granell.pdf, 2004.

Hanna, S. R., Strimaitis, D. G., and Chang, J. C.: Hazard response modeling uncertainty (A quantitative method), 1991.

Hanna, S. R., Chang, J. C., and Strimaitis, D. G.: Hazardous gas model evaluation with field observations, Atmos. Environ., 27, 2265–2285, 1993.

Hao, J. M., Wu, Y., Fu, L. X., He, D. Q., and He, K. B.: Source contributions to ambient concentrations of CO and NOx in the urban area of Beijing, J. Environ. Sci. Heal. A – Toxic/Hazard. Subst. Environ. Eng., 36, 215–228, 2001.

Hirtl, M. and Baumann-Stanzer, K.: Evaluation of two dispersion models (ADMS-Roads and LASAT) applied to street canyons in Stockholm, London and Berlin, Atmos. Environ., 41, 5959–5971, 2007.

Hu, F.: Turbulence interval and atmospheric boundary layer [D], Ph.D dissertation, Institute of Atmospheric Physics, Chinese Academy of Sciences, 1994 (in Chinese).

Kenty, K. L., Poor, N. D., Kronmiller, K. G., McClenny, W., King, C., Atkeson, T., and Campbell, S. W.: Application of CALINE4 to roadside NO/NO_2 transformations, Atmos. Environ., 41, 4270–4280, 2007.

Khoder, M. I.: Diurnal, seasonal and weekdays-weekends variations of ground level ozone concentrations in an urban area in greater Cairo, Environ. Monit. Assess., 149, 349–362, 2009.

Kukkonen, J., Valkonen, E., Walden, J., Koskentalo, T., Aarnio, P., Karppinen, A., Berkowicz, R., and Kartastenpaa, R.: A measurement campaign in a street canyon in Helsinki and

comparison of results with predictions of the OSPM model, Atmos. Environ., 35, 231–243, 2001.
Levitin, J., Harkonen, J., Kukkonen, J., and Nikmo, J.: Evaluation of the CALINE4 and car-fmi models against measurements near a major road, Atmos. Environ., 39, 4439–4452, 2005.
Liu, J., Zhang, X. L., Xie, P., Dong, F., Ouyang, J., and Wang, Z. F.: The variation characteristics of trace reactive gases at Shangdianzi regional background monitoring station, Environ. Chem. (in Chinese), 26(5), 693–698, 2007.
Liu, J., Zhang, X. L., Xu, X. F., and Xu, H. H.: Comparison analysis of variation characteristics of SO_2, NO_x, O_3 and $PM_{2.5}$ between rural and urban areas, Beijing, Environ. Science, 29(4), 1059–1065, 2008 (in Chinese).
Liu, J., Zhang, X. L., Zhang, X. C., and Tang, J.: Surface ozone characteristics and the correlated factors at Shangdianzi atmospheric background monitoring station, Res. Environ. Sciences, 19(4), 19–25, 2006 (in Chinese).
Liu, X. M., Hu, F., and Li, L.: Analyses on the characteristics of Beijing summer urban heat island and its meteorological fields (in Chinese), J. Grad. School. Chinese. Acad. Sci., 23, 70–76, 2006.
Lu, L. H., Bian, L. G., Cheng, Y. J., Gao, Z. Q., and Wang, Y.: Meteorological Characteristics of the ground layer in Beijing in winter, J. Appl. Meteorol. Science, 13, 34–42, 2002 (in Chinese).
McHugh, C. A., Carruthers, D. J., and Edmunds, H. A.: ADMS-Urban: An air quality management system for traffic, domestic and industrial pollution, Int. J. Environ. Pollut., 8, 666–674, 1997.
McHugh, C., Carruthers, D., and Sheng, X. Y.: Using ADMS models for air quality assessment and management in China, Cambridge Environmental Research Consultants (CERC), Chinese. J. Popul. Resour. Environ., 3, 3–10, 2005.
Miao, S. G., Chen, F., Margaret, A. L., Mukul, T., Li, Q. C., and Wang, Y. C.: An observational and modeling study of characteristics of urban heat island and boundary layer structures in Beijing, J. Appl. Meteorol. Clim., 48, 484–501, 2008.
Ministry of Environmental Protection of China, Guidelines for environmental impact assessment – atmospheric environment, 24 pp., 2009.
Murphy, J. G., Day, D. A., Cleary, P. A., Wooldridge, P. J., Millet, D. B., Goldstein, A. H., and Cohen, R. C.: The weekend effect within and downwind of Sacramento - Part 1: Observations of ozone, nitrogen oxides, and VOC reactivity, Atmos. Chem. Phys., 7, 5327–5339, 2007,

http://www.atmos-chem-phys.net/7/5327/2007/.
NARSTO: An assessment of tropospheric ozone pollution: A North American perspective, The NARSTO Synthesis Team, Palo Alto, CA, 2000.
NASA: Aura/OMI Tropospheric NO2: Area around Beijing, China, http://aura.gsfc.nasa.gov/science/china.html, 2009.
Olesen, H. R.: Ten years of harmonization activities: past, present, and future, 7th Int. Conf. on Harmonisation within Atmospheric Dispersion Modelling for Regulatory Purposes, Belgirate, Italy, National Environmental Research Institute, Roskilde, Denmark, www.harmo.org, 2001.
Riddle, A., Carruthers, D., Sharpe, A., McHugh, C., and Stocker, J.: Comparisons between fluent and ADMS for atmospheric dispersion modelling, Atmos. Environ., 38, 1029–1038, 2004.
Sadanaga, Y., Shibata, S., Hamana, M., Takenaka, N., and Bandow, H.: Weekday/weekend difference of ozone and its precursors in urban areas of Japan, focusing on nitrogen oxides and hydrocarbons, Atmos. Environ., 42, 4708–4723, 2008.
Sharma, S. and Chandra, A.: Simulation of air quality using an ISCST3 dispersion model, Clean-Soil. Air. Water, 36, 118–124, 2008.
Song, Y., Zhang, Y. H., Xie, S. D., Zeng, L. M., Zheng, M., Salmon, L. G., Shao, M., and Slanina, S.: Source apportionment of $PM_{2.5}$ in Beijing by positive matrix factorization, Atmos. Environ., 40, 1526–1537, 2006.
Tang, W. Y., Zhao, C. S., Geng, F. H., Peng, L., Zhou, G. Q., Gao, W., Xu, J. M., and Tie, X. X.: Study of ozone "weekend effect" in Shanghai, Sci. China Ser. D, 51, 1354–1360, 2008.
Vardoulakis, S., Valiantis, M., Milner, J., and Apsimon, H.: Operational air pollution modelling in the UK-Street canyon applications and challenges, Atmos. Environ., 41, 4622–4637, 2007.
Venkatram, A., Karamchandani, P.O., Pai, P., Goldstein, R.: The development and application of a simplified ozone modelling system, Atmos. Environ., 28, 3665–3678, 1994.
Wang, B. G., Zhang, Y. H., Wu, Z. Q., and Chan, L. Y.: Tunnel test for motor vehicle emission factors in Guangzhou, Res. Environ. Sci., 14, 13–16, 2001.
Wang, L. J., Parker, D. B., Parnell, C. B., Lacey, R. E., and Shaw, B. W.: Comparison of Calpuff and ISCST3 models for predicting downwind odor and source emission rates, Atmos. Environ., 40, 4663–4669, 2006.
Wang, T. and Xie, S. D.: Assessment of traffic-related air pollution in the urban streets before and during the 2008 Beijing Olympic Games traffic control period, Atmos. Environ., 43, 5682–5690, 2009.

Wang, X., Westerdahl, D., Chen, L. C., Wu, Y., Hao, J. M., Pan, X. C., Guo, X. B., and Zhang, K. M.: Evaluating the air quality impacts of the 2008 Beijing Olympic Games: On-road emission factors and black carbon profiles, Atmos. Environ., 43, 4535–4543, 2009a.
Wang, X. S. and Li, J. L.: The contribution of anthropogenic hydrocarbons to ozone formation in Beijing areas, China Environ. Sci., 22, 501–505, 2002 (in Chinese).
Wang, X. S., Li, J. L., Zhang, Y. H., Xie, S. D., and Tang, X. Y.: Ozone source attribution during a severe photochemical smog episode in Beijing, China, Sci. China. Ser. B-Chem., 52, 1270–1280, 2009.
Wang, Y., Hao, J., McElroy, M. B., Munger, J. W., Ma, H., Chen, D., and Nielsen, C. P.: Ozone air quality during the 2008 Beijing Olympics: effectiveness of emission restrictions, Atmos. Chem. Phys., 9, 5237-5251, 2009b, http://www.atmos-chem-phys.net/9/5237/2009/.
Westerdahl, D., Wang, X., Pan, X. C., and Zhang, K. M.: Characterization of on-road vehicle emission factors and microenvironmental air quality in Beijing, China, Atmos. Environ., 43, 697–705, 2009.
WHO: World Health Organization Air Quality Guidelines Global Update, http://www.euro.who.int/air/activities/20050222_2, 2005.
Willmott, C. J.: Some comments on the evaluation of model performance, B. Am. Meteor. Soc., 63, 1309–1313, 1982.
Xie, S. D., Liu, Z., Chen, T., and Hua, L.: Spatiotemporal variations of ambient PM_{10} source contributions in Beijing in 2004 using positive matrix factorization, Atmos. Chem. Phys., 8, 2701–2716, 2008, http://www.atmos-chem-phys.net/8/2701/2008/.
Ying, G. X., Ma, J., and Xing, Y.: Comparison of air quality management strategies of PM_{10}, SO_2, and NO_x, by an industrial source complex model in Beijing, Environ. Prog., 26, 33–42, 2007.
Yura, E. A., Kear, T., and Niemeier, D.: Using CALINE dispersion to assess vehicular $PM_{2.5}$ emissions, Atmos. Environ., 41, 8747–8757, 2007.
Zhang, H. S. and Chen, J. Y.: Estimation of aerodynamic parameters on nonsingle horizontal homogeneous underlying surface, J. Appl. Meteor. Sci., 8(3), 310–315, 1997 (in Chinese).

Table 1. Determination of representative parameters for the model set up.

Parameters	Value
Surface roughness (m)	1.0
Latitude of the modelling area (°)	40
Minimum Monin-Obukhov length (m)	30
Pollutants included	NO_x, NO_2, CO, PM_{10} and O_3
Number of grids	10000
Height of concentrations to be calculated (m)	1.5

ACPD

10, 5135–5184, 2010

Table 2. Emission factors (g/km) for passenger cars, light duty vehicles, heavy duty vehicles and buses at a typical urban running speed of 20 km/h in Beijing, calculated by COPERT and from literature reports.

	PM_{10}	CO	NO_x	VOC
Passenger cars	0.015[a]	5.99	0.44	0.35
Light duty vehicles	0.015[a]	11.28	0.82	0.47
Heavy duty vehicles	2.94[a]	2.22	2.72	0.91
Buses	2.94[a]	4.76	10.54	0.87

[a] from Wang et al. (2001), as COPERT assumes gasoline vehicles do not emit particles.

ACPD
10, 5135–5184, 2010

Table 3. Statistical evaluation of model performance based on hourly predictions and observations at CGZ monitoring site.

	CO	PM_{10}	NO_2	O_3
Observed mean ($\mu g/m^3$)	1214.2	84.1	52.3	52.7
Predicted mean ($\mu g/m^3$)	1459.6	84.8	46.5	38.3
FB (ideal value: 0)	−0.22	−0.01	0.12	0.31
FAC2 (ideal value: 100%)	0.71	0.65	0.69	0.50
NMSE (ideal value: 0)	0.76	0.54	0.33	0.71
NMSEs (ideal value: 0)	0.05	0.00	0.01	0.10
MG (ideal value: 1)	0.92	0.81	1.07	3.33
VG (ideal value: 1)	1.57	2.27	1.42	4.51
R (ideal value: 1)	0.34	0.45	0.56	0.68

ACPD
10, 5135–5184, 2010

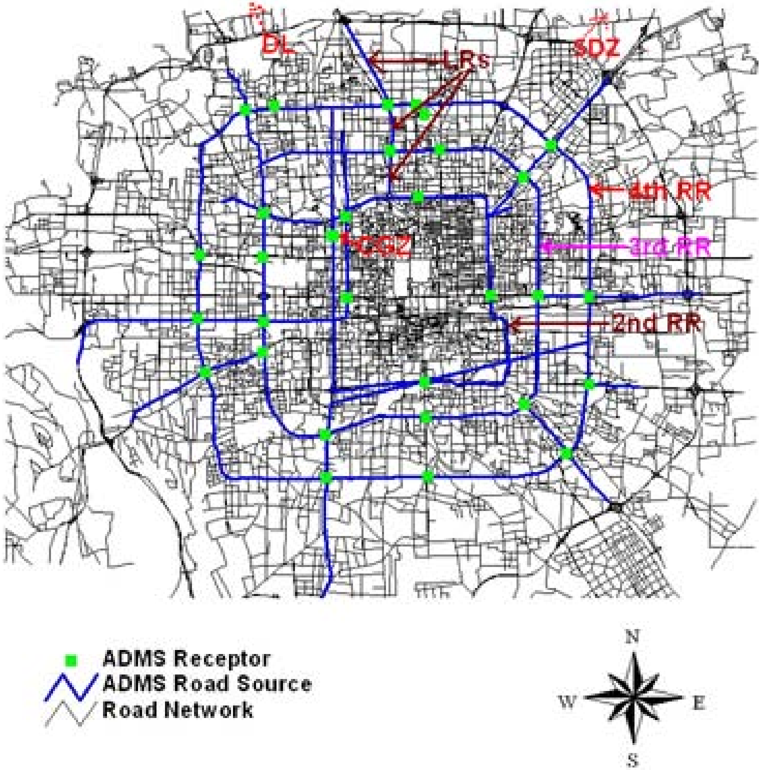

Fig. 1. Map of the road network of UAB, road sources of RR and LRs, CGZ, DL and SDZ air quality monitoring sites, and representative receptors distributed in the study domain.

ACPD
10, 5135–5184, 2010

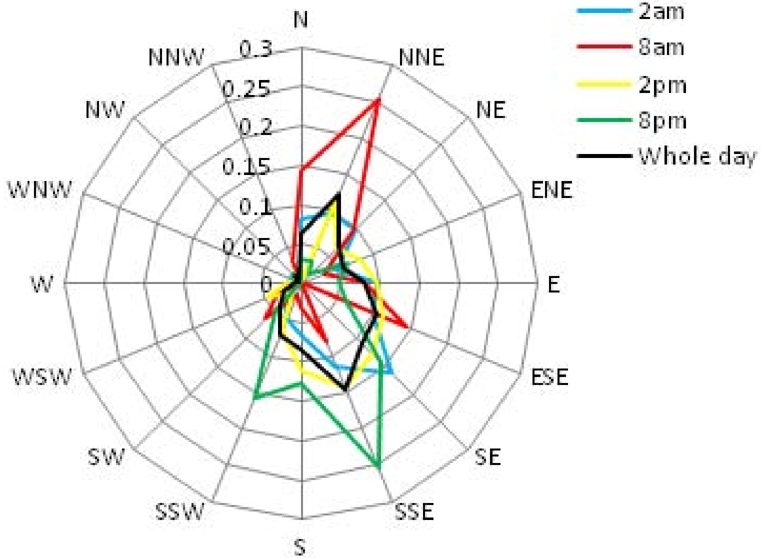

Fig. 2. Wind roses of wind directions at 2 a.m., 8 a.m., 2 p.m., 8 p.m. and the whole day from July to September 2008. The radius indicates the frequency of wind observed in each direction.

ACPD
10, 5135–5184, 2010

A modelling study of air quality impact of odd-even day traffic restriction scheme

H. Cai and S. D. Xie

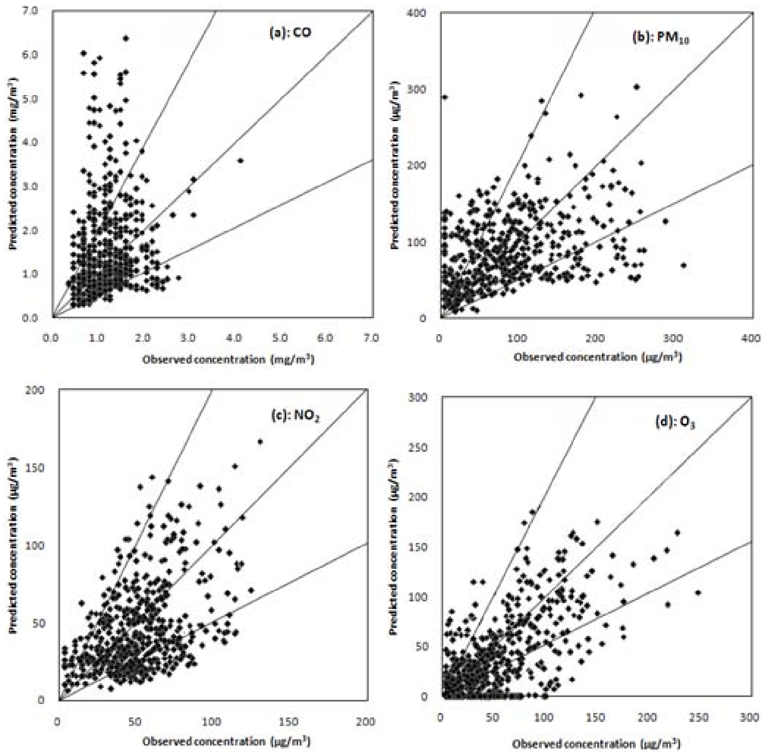

Fig. 3. Scatter plot comparison between observed and predicted hourly concentrations of **(a)** CO, **(b)** PM_{10}, **(c)** NO_2 and **(d)** O_3 for the periods of 10–20 July and 10–20 August 2008, at the CGZ air quality monitoring site, for the evaluation of ADMS-Urban model. The lines showing an agreement of predictions and observations by a factor of two are also presented.

ACPD
10, 5135–5184, 2010

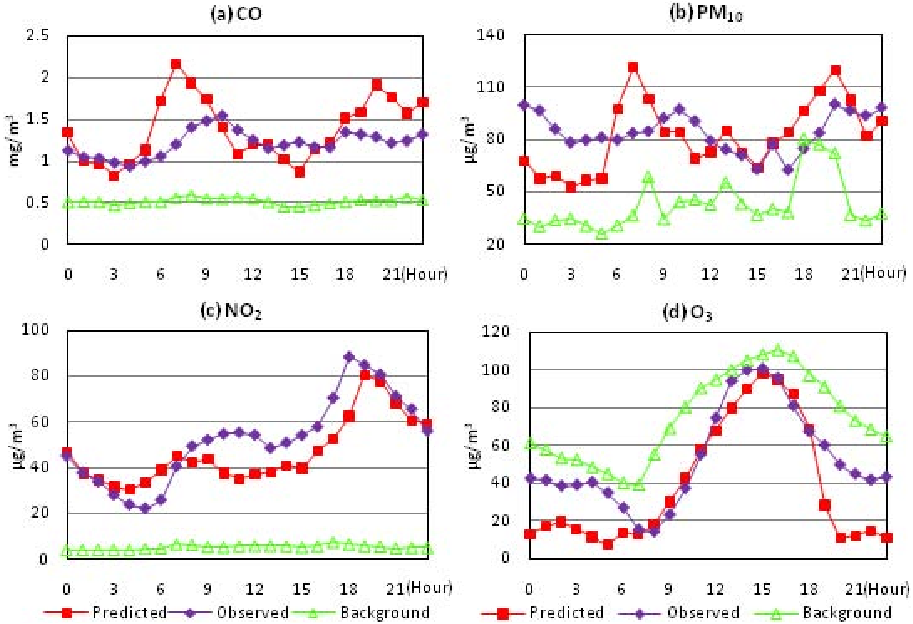

Fig. 4. Model performance on time-of-the-day, in comparison with the diurnal profiles of observed and background concentrations for **(a)** CO; **(b)** PM_{10}; **(c)** NO_2 and **(d)** O_3.

ACPD
10, 5135–5184, 2010

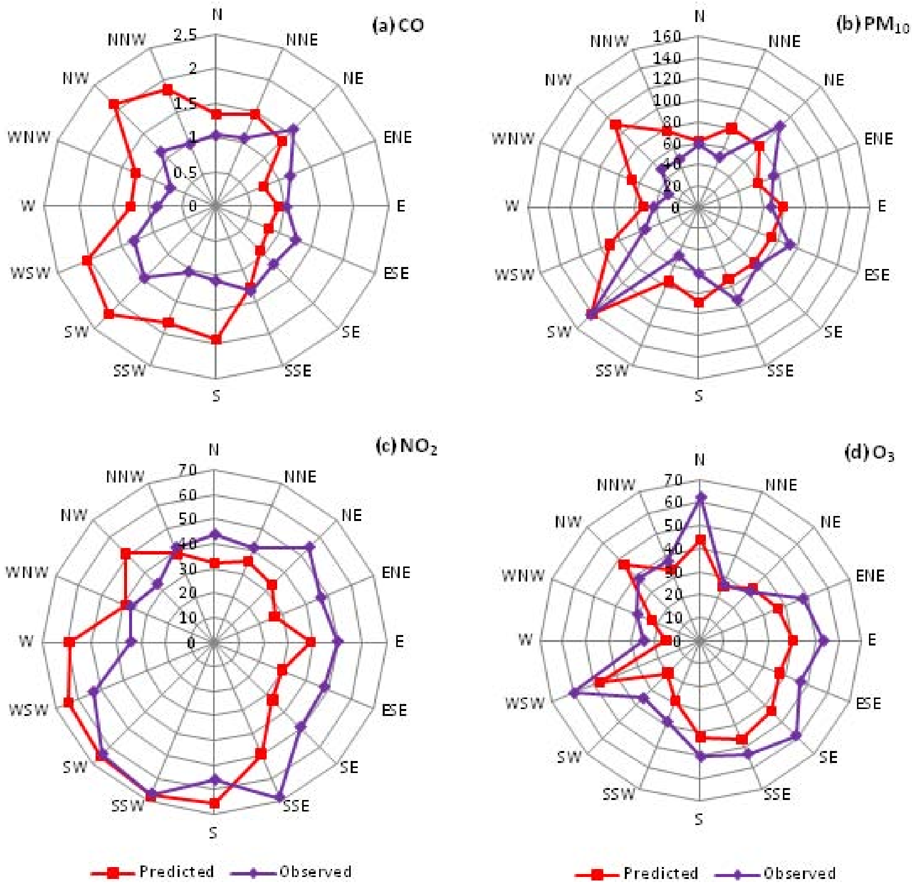

Fig. 5. Comparison of mean predicted and observed pollutant concentration roses for **(a)** CO, **(b)** PM_{10}, **(c)** NO_2 and **(d)** O_3 in different wind directions for the periods of 10–20 July and 10–20 August 2008, at the CGZ air quality monitoring site.

ACPD
10, 5135–5184, 2010

A modelling study of air quality impact of odd-even day traffic restriction scheme

H. Cai and S. D. Xie

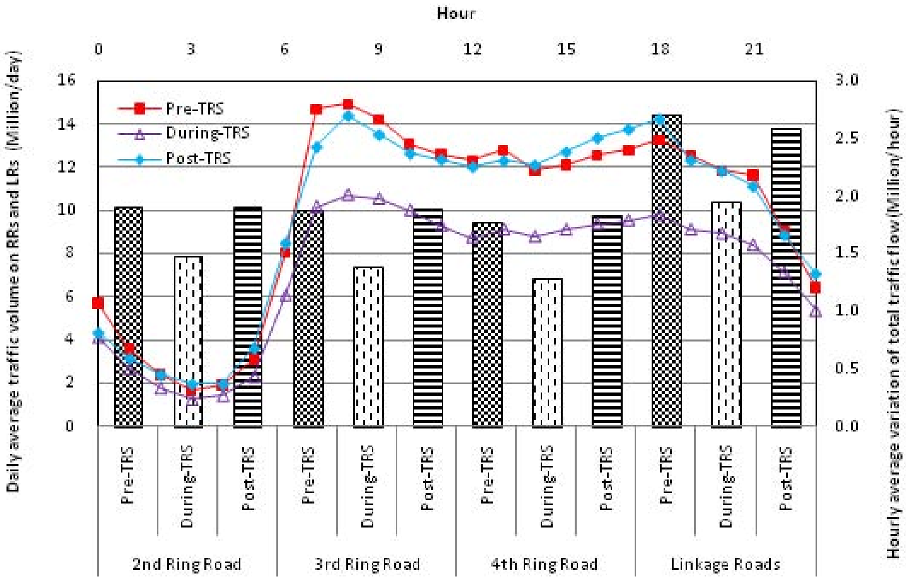

Fig. 6. Comparison of traffic flows on 2nd RR, 3rd RR, 4th RR and the LRs on daily average, and diurnal variation of total traffic flow on hourly average for the pre-TRS, during-TRS and post-TRS periods, respectively.

ACPD
10, 5135–5184, 2010

Title Page
Abstract Introduction
Conclusions References
Tables Figures
◀ ▶
Back Close
Full Screen / Esc
Printer-friendly Version
Interactive Discussion

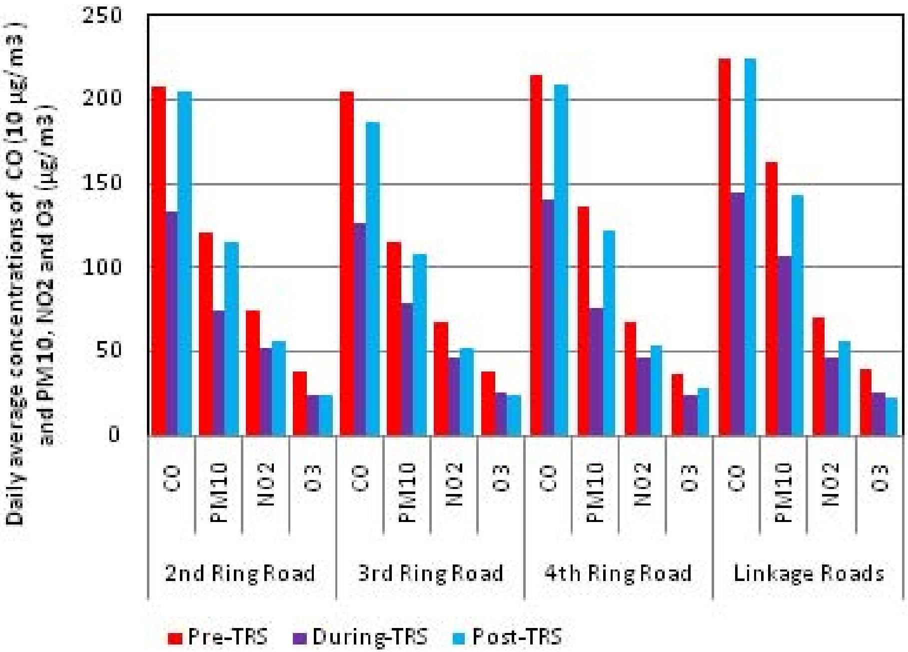

Fig. 7. Comparison of daily average concentrations of CO, PM_{10}, NO_2 and O_3 on different road types for the pre-TRS, during-TRS and post-TRS periods.

ACPD

10, 5135–5184, 2010

A modelling study of air quality impact of odd-even day traffic restriction scheme

H. Cai and S. D. Xie

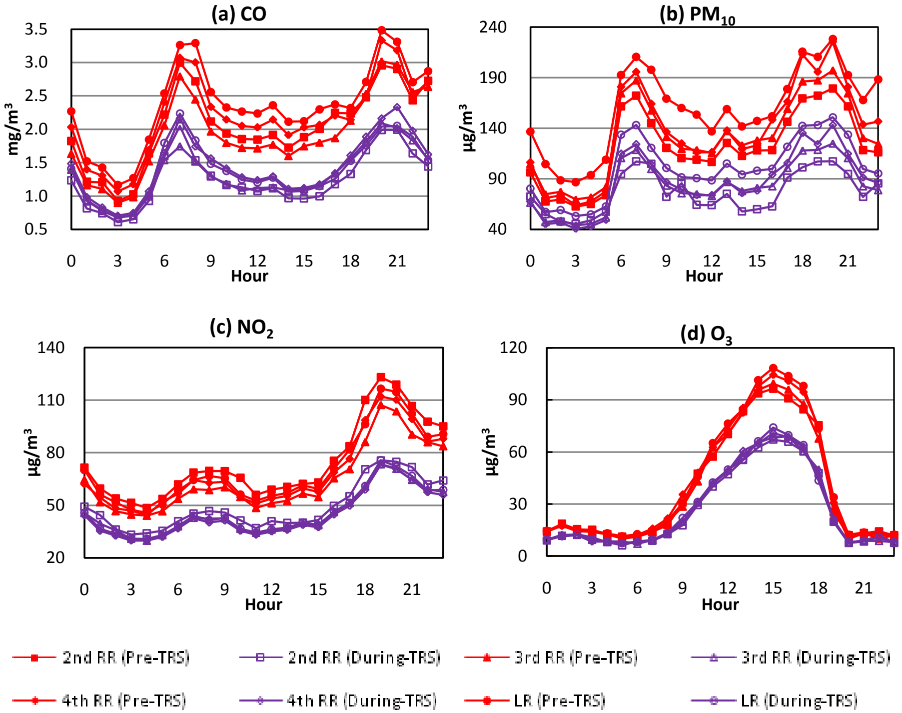

Fig. 8. Comparison of diurnal variations of hourly concentrations of **(a)** CO; **(b)** PM_{10}; **(c)** NO_2 and **(d)** O_3 on 2nd, 3rd, 4th RR and the LRs for the pre- and during- TRS periods.

ACPD

10, 5135–5184, 2010

A modelling study of air quality impact of odd-even day traffic restriction scheme

H. Cai and S. D. Xie

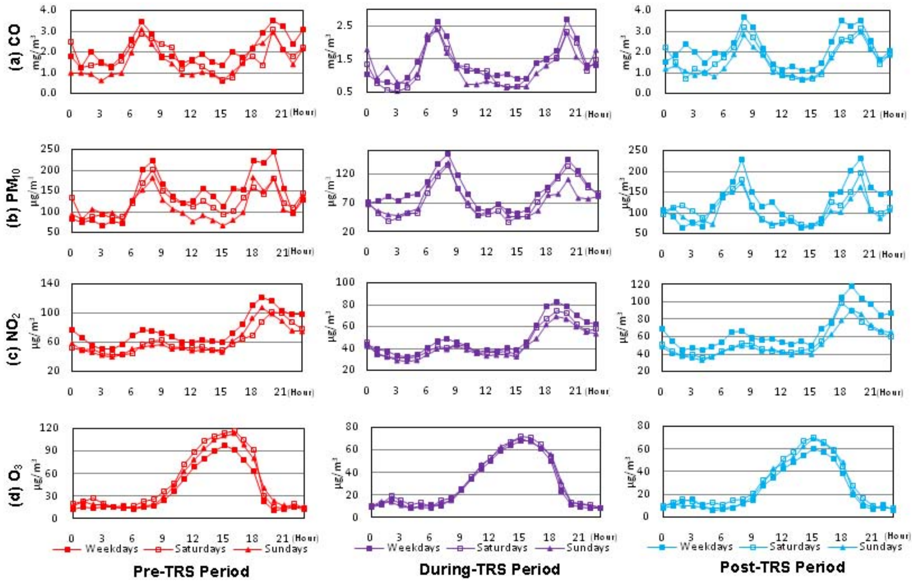

Fig. 9. Day-of-the-week variations of **(a)** CO; **(b)** PM_{10}; **(c)** NO_2 and **(d)** O_3 diurnal profiles in response to the implementation of the TRS policy.

ACPD
10, 5135–5184, 2010

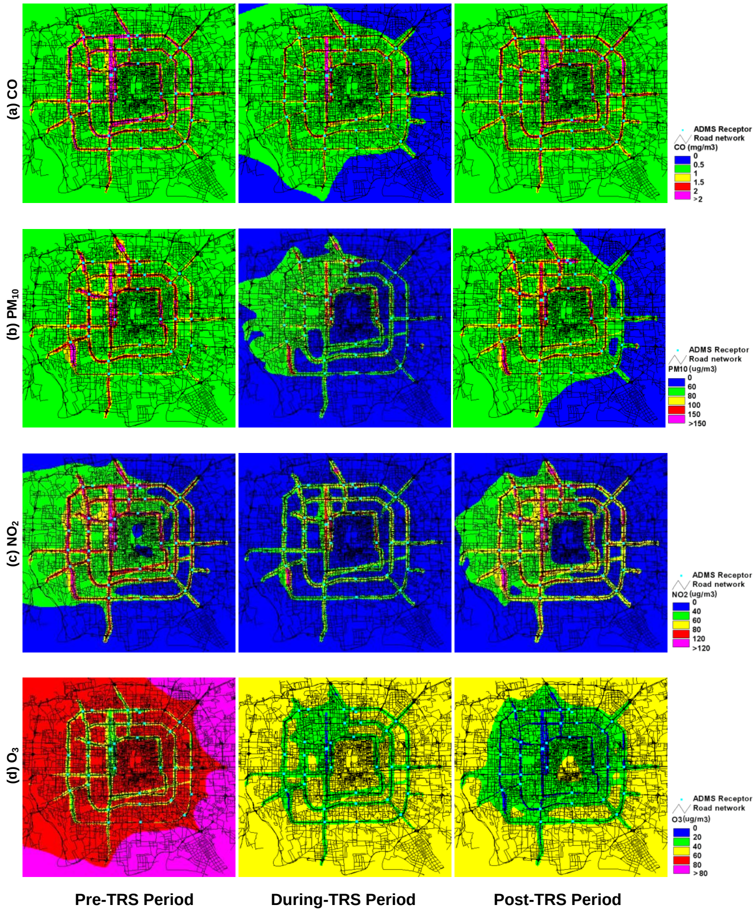

Fig. 10. Spatial distribution of **(a)** CO; **(b)** PM_{10}; **(c)** NO_2 and **(d)** O_3 concentrations on daily average for pre-, during- and post-TRS periods, and the spatial variation of regional air quality impacts in response to the TRS policy.

ACPD
10, 5135–5184, 2010

A modelling study of air quality impact of odd-even day traffic restriction scheme

H. Cai and S. D. Xie

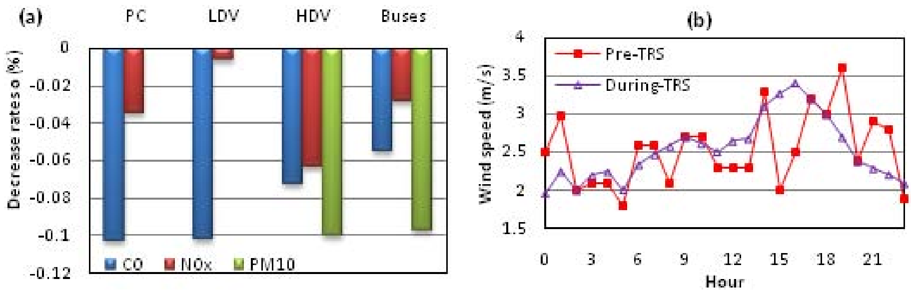

Fig. 11. Air quality impacts during the Games of **(a)**: Reduction rates of emission factors of CO, PM_{10} and NO_x from various vehicle types resulting from the raise of running speed from 20 km/h to 23 km/h, calculated by COPERT model; **(b)** Variation of wind speed (m/s) on hourly average for the pre-TRS and during-TRS periods.

ACPD
10, 5135–5184, 2010